energies

MDPI

Article

Hybrid Artificial Intelligence Model for Reliable Decision Making in Power Transformer Maintenance Through Performance Index

Vinícius Faria Costa Mendanha [1], André Pereira Marques [2], Lucas Santos de Aguiar [1], Juliermy Junio Pacheco dos Santos [1], Álisson Assis Cardoso [1] and Cacilda de Jesus Ribeiro [1,*]

[1] School of Electrical, Mechanical and Computer Engineering, Federal University of Goiás, Goiânia 74605-010, Brazil; vinicius.fcfariacosta@gmail.com (V.F.C.M.); santosaguiar2010@gmail.com (L.S.d.A.); juliermy_junio@discente.ufg.br (J.J.P.d.S.); alsnac@ufg.br (Á.A.C.)

[2] Electrical Engineering, Federal Institute of Goiás, Goiânia 74055-110, Brazil; ap.marques@ifg.edu.br

* Correspondence: cacilda@ufg.br; Tel.: +55-62-99938-8801

Abstract

The preventive maintenance of power transformers is essential to ensure their reliability and is supported by efficient predictive techniques and accurate diagnostics. In this context, the objective of this work is to present a hybrid Artificial Intelligence (AI) model for reliable decision making in transformer maintenance based on performance index monitoring. The innovation lies in the application of Monte Carlo filters to monitor the operational state of transformers combined with a novel clustering strategy. The used methodology includes the development of an algorithm for outlier removal in the historical series of each predictive technique as well as the implementation of stochastic filters to forecast the overall operational condition. The results demonstrate the robustness and effectiveness of the developed model. This work contributes a new AI-based strategy for supporting preventive maintenance decisions, enabling precise and individualized actions for each piece of equipment, with broad applicability to companies in the electrical power sector.

Keywords: artificial intelligence; performance index; power transformers; preventive maintenance; reliability

Academic Editor: Adolfo Dannier

Received: 12 August 2025
Revised: 26 August 2025
Accepted: 10 September 2025
Published: 16 September 2025

Citation: Mendanha, V.F.C.; Marques, A.P.; de Aguiar, L.S.; dos Santos, J.J.P.; Cardoso, Á.A.; Ribeiro, C.d.J. Hybrid Artificial Intelligence Model for Reliable Decision Making in Power Transformer Maintenance Through Performance Index. *Energies* **2025**, *18*, 4924. https://doi.org/10.3390/en18184924

1. Introduction

Power transformers are frequently subjected to diagnostic tests aimed at predicting the operational condition of their components [1]. These procedures produce datasets for each predictive technique, typically composed of the normalized performance index (ranging from 0 to 1 pu), measured at specific time intervals (in days, months, or years), along with the operational status classified as either operation or intervention. However, effective analytical strategies are needed to process these datasets in a way that allows maintenance specialists to objectively and comprehensively assess the overall equipment performance by integrating the outputs of all techniques. This integrated analysis supports improved decision making and enhances the reliability of the power system. Although the AI model developed in this work is general and applicable to any power transformer, this paper focuses on case studies involving high-voltage power transformers immersed in mineral-insulating oil.

Among the most used predictive techniques for evaluating the paper–oil system are Dissolved Gas Analysis (DGA), Degree of Polymerization (DP), and Physicochemical Tests

(PC), all of which are widely employed in the power sector to detect incipient faults in transformers [2,3]. In addition, electrical tests are performed to assess the integrity of the transformer and its components, including Insulation Resistance (ET_IR), Insulation Power Factor (ET_PF), Turns Transformation Ratio (ET_TTR), Winding Resistance (ET_WR), Low Voltage Excitation Current (ET_LVEC), and Capacitance and Tangent Delta of Condenser Bushings (ET_CB).

However, potential outliers in the sample data, arising from electromagnetic interference, environmental fluctuations, sampling inconsistencies, or calibration errors in data acquisition equipment, can hinder the consistent interpretation of predictive technique results. Such discrepancies introduce bias into the analysis, complicating the identification of actual operational patterns. As a result, diagnostic quality may be compromised, directly impacting maintenance decisions, especially regarding the optimal timing of interventions to prevent catastrophic failures and unplanned service interruptions in utility operations.

Thus, it is essential to employ tools capable of detecting outliers in these datasets. To this end, several solutions based on machine learning algorithms have been proposed for analyzing predictive technique data, including the Local Outlier Factor (LOF), K-Nearest Neighbors (KNN), Isolation Forest (IF), Gaussian Mixtures, and Density-Based Spatial Clustering of Applications with Noise (DBSCAN) [4–6]. However, these algorithms exhibit some limitations: their accuracy is highly sensitive to the volume of data and the number of neighbors selected. Moreover, for large datasets, they tend to impose a high computational cost.

With regard to the prediction of power transformer performance during operation, several tools have been proposed for continuous monitoring. One such approach involves a methodology based on Analytic Hierarchy Process (AHP) multicriteria analysis, which was developed to assess the operating conditions of power transformers by considering both their lifespan characteristics (failure risk factor) and their systemic importance (impact factor) within the electrical network [7]. Similarly, another diagnostic methodology was proposed to estimate the operational state of transformers by incorporating the influence of harmonic distortions into the calculation of the health index [8].

Moreover, a finite-state machine-based diagnostic model for power transformers in substations was proposed by [9], in which chromatographic, physicochemical, and electrical analyses are used to determine operational states and to recommend preventive maintenance actions. In the context of applying artificial intelligence to preventive maintenance processes, several studies have been conducted. For instance, machine learning has been employed to estimate the Degree of Polymerization (DP), which is a key indicator of transformer aging [10]. In addition, prognostics and the health management of power transformers have been explored using a whale-inspired hybrid optimization algorithm [11]. In the domain of dissolved gas analysis (DGA), gas forecasting has been investigated through mixed-kernel support vector regression (SVR) combined with genetic algorithms [12]. Furthermore, expertise-guided machine learning (EGML) has been applied to diagnose internal faults in power transformers, using backpropagation neural networks (BPNNs) enhanced by genetic algorithms (GAs) and Memetic Evolutionary Algorithms (MEAs) [13].

Advances in artificial intelligence research have also made significant contributions to the modeling of predictive processes in dynamic systems. For example, an extensive empirical comparison of time series anomaly detection algorithms was conducted, many of which rely on forecasting mechanisms to model expected behavior and detect deviations [14]. The study highlights how prediction-based techniques, including deep learning architectures such as Long Short-Term Memory (LSTM) networks and autoencoders, can effectively support maintenance strategies by anticipating performance

degradation. Additionally, causal discovery methods tailored for time series data are designed, offering new perspectives on identifying structural dependencies in dynamic environments, presenting a comprehensive survey and an evaluation of algorithms designed to uncover causal relationships across time, including constraint-based, score-based, and functional-model-based approaches [15]. These methods can be instrumental in preventive maintenance scenarios by enabling systems not only to forecast future behavior but also to infer underlying causal mechanisms responsible for degradation. This causal observation can augment traditional prediction strategies, such as those based on recurrent neural networks or forecasting filters, like Kalman filters and particle filters, by providing more robust explanations and improving interpretability in model-based maintenance planning.

Furthermore, stochastic modeling approaches based on D-spectrum theory and failure counting processes provide a probabilistic foundation for reliability assessment in complex systems [16]. Performance improvements from time series data augmentation have also been observed in small-sample signal recognition scenarios, highlighting the benefits of enhanced data under constraints typical of industrial monitoring datasets [17]. This scenario is particularly common in maintenance environments, as utilities often have limited historical data for certain types of equipment due to infrequent failures, incomplete records, or newly deployed assets. A hierarchical deep learning strategy combining syntactic and semantic graph representations has also been proposed for defect prediction in source code, offering transferable insights for degradation modeling through enriched feature learning [18]. These studies reinforce the relevance of AI-based methods in reliability engineering and point to the continued demand for interpretable and data-efficient models under uncertainty.

In that way, the objective of this study is to present a hybrid artificial intelligence model aimed at supporting assertive decision making in power transformer maintenance that is grounded in performance monitoring data. The model is structured in the following stages:

- Preprocessing stage: the accuracy of two unsupervised AI algorithms, the Local Outlier Factor (LOF) and Isolation Forest (IF), is assessed using expert-labeled data. Their outputs are compared to a novel outlier detection method developed in this work, which removes inconsistencies based on historical neighborhood consistency while preserving critical anomalies relevant to maintenance decisions.
- Output stage: maintenance recommendations are generated based on the classification of the performance index into five categories (A to E), reflecting the equipment's condition. Forecasting is then conducted using the AD-SIS and AD-Bootstrap frameworks, which estimate the future evolution of the performance index by modeling dynamic systems under uncertainty.

The main contribution of this study lies in the development of two custom Monte Carlo-based filtering frameworks (AD-Bootstrap and AD-SIS) specifically designed to handle noisy, incomplete, and irregularly sampled conditions, enabling reliability-centered probabilistic forecasting of equipment behavior. The proposed approach integrates unsupervised learning for outlier detection, temporal clustering based on intervention effectiveness, and Monte Carlo filtering, applied to real operational datasets. In contrast to previous models that analyze predictive techniques in isolation, this methodology seeks to consolidate nine predictive techniques into a unified and interpretable decision-making framework. By structuring these elements within a single model, the framework is expected to support a more informed analysis of degradation trends and assist utility professionals in planning maintenance actions with greater confidence.

2. Methodology

In the methodology adopted in this study, a computational tool was developed to apply the classification criteria for the power transformer performance index, as defined in Table 1 [19], based on the worst predicted value at each time instant.

Table 1. Recommended actions based on the predicted performance index classification of the power transformer [19].

Performance Index (y)	Classification	Recommended Actions
$0.80 \leq y \leq 1.00$	A (Excellent)	The equipment should continue operating normally.
$0.65 \leq y < 0.80$	B (Good)	The equipment should continue operating, monitoring the evolution of results in upcoming records.
$0.50 \leq y < 0.65$	C (Marginal)	The equipment should be investigated, and additional tests should be conducted in the short term to confirm results and trends.
$0.35 \leq y < 0.50$	D (Poor)	Planning for the equipment's removal from operation for internal inspection, fault localization, and correction.
$0.00 \leq y < 0.35$	E (Very Poor)	The equipment must be immediately removed from operation for internal inspection, fault identification, and correction.

The classification from Table 1 [19] considers a total of nine tests, namely Dissolved Gas Analysis (DGA), Physicochemical Tests (PC), Degree of Polymerization (DP), Electrical Tests of Low Voltage Excitation Current (ET_LVEC), Insulation Power Factor (ET_PF), Turns Transformation Ratio (ET_TTR), Insulation Resistance (ET_IR), Winding Resistance (ET_WR), and Capacitance and Tangent Delta of Condenser Bushings (ET_CB). These tests represent the main predictive techniques used in transformer diagnostics, covering chemical, electrical, and physical indicators of degradation, and thus ensure a comprehensive assessment of equipment condition [1,19,20].

2.1. Artificial Intelligence Algorithms for Identifying Outliers

Initially, during the data preprocessing stage, two Artificial Intelligence algorithms, the Local Outlier Factor (LOF) and Isolation Forest (IF), assess the performance history of the power transformer throughout its operation, considering each set of the nine predictive techniques. Individually, the tool performs a clustering based on the effectiveness of the intervention. To this end, at each observed time instant, t_i, with $i \in [1, n]$ and n being the number of samples for each technique, the status is monitored. If an intervention is recorded at time t_i, the algorithm analyzes the performance index of the transformer $y(t_i)$. If it shows improvement compared to the previous sample, $y(t_{i-1})$, a new cluster $\mathcal{C}$ is initiated. Otherwise, it is understood that the maintenance was not effective for the evaluated predictive technique, i.e., it did not result in performance improvement for that set, and the subsequent data remain within the previous cluster, according to the decision rule defined in (1).

$$\mathcal{C}(y(t_i)) = \begin{cases} \mathcal{C}_{\text{new}}, & \text{if } y(t_i) > y(t_{i-1}) \\ \mathcal{C}_{\text{previous}}, & \text{otherwise} \end{cases} \tag{1}$$

At the end of this stage, the sets of each predictive technique may be divided into subsets, in which the data exhibit well-defined temporal coherence, as the operational status is taken into account in the assessment of power transformer performance. Then, Artificial Intelligence algorithms are executed for the clusters. The first algorithm is the Local Outlier Factor (LOF), which is an unsupervised tool for outlier detection based on density and neighborhood. For each instance $x = (y_j, t_j)$, with $j \in [1; n']$ and n' being

the total number of elements in the cluster, the Euclidean distance $d_k(x)$ between x and its k-nearest neighbors is computed [21,22]. Additionally, $\mathcal{M}(x)$ represents the set of training instances in the neighborhood of x, and for each $s \in \mathcal{M}(x)$, the distance $d_k(s)$ is determined. By comparing $d_k(x)$ with the mean value of $d_k(s)$ for each s, the Local Outlier Factor (LOF(x)) is calculated according to (2), where $|\mathcal{M}(x)| = k$. If the resulting value is close to 1, the instance x is not considered an outlier; otherwise, it is likely to be an outlier.

$$\text{LOF}(x) = \frac{d_k(x) \cdot |\mathcal{M}(x)|}{\sum_{s \in \mathcal{M}(x)} d_k(s)} \tag{2}$$

The second algorithm used for outlier detection is Isolation Forest (IF). It generates random trees to partition the data within each cluster and computes the number of nodes required to isolate each training vector [23]. Thus, outliers are identified as the vectors with the shortest average path lengths for isolation, based on the principle that they tend to be more densely distributed and clustered than anomalies, requiring more nodes to be isolated. The anomaly score, denoted by score(x), for each instance is computed in (3), where $E[h(x)]$ represents the expected average path length to isolate point x in the forest, and $c(\psi)$ is the average path length value for a dataset of size ψ, which is used as a normalizing factor [23].

$$\text{score}(x) = 2^{-\frac{E[h(x)]}{c(\psi)}} \tag{3}$$

Finally, the expected average path length $h(x)$ required to isolate a point in a dataset with n elements, denoted as $c(n)$, is computed for n samples in (4), where $H(n)$ represents the harmonic number of the n-th term. For large values, $H(n) = \ln(n) + 0.577$ [23].

$$c(n) = 2H(n-1) - \frac{2(n-1)}{n} \tag{4}$$

Based on the values obtained in (3) and (4), the following conclusions are drawn:

- If $E[h(x)] = c(n)$, then score$(x) = 0.5$, indicating nominal behavior for x.
- If $E[h(x)] \to \infty$, then x is not isolated, meaning it exhibits nominal behavior.
- If $E[h(x)]$ is small compared to $c(n)$, then score(x) tends to one, indicating that x is an outlier.

After the outlier detection and removal stage, the data from each predictive technique are compared at each time instant, and the overall performance index $y(t)$ is obtained as the minimum value among all individual indices at that time. This conservative criterion prioritizes the worst-performing predictive component at each instant, aligning with preventive maintenance strategies by emphasizing early intervention based on the most critical signal.

2.2. New Method Developed for Identifying Outliers

The algorithm developed (AD) in this work for detecting and eliminating outliers is based on two main assumptions:

1. The performance index of power transformers does not increase in the absence of maintenance or intervention. Thus, any spontaneous increment is interpreted as an undue improvement, i.e., for a given sample i, where $y(t_i)$ and $y(t_{i-1})$ denote the performance index at times t_i and t_{i-1}, respectively, as expressed in (5).

$$\Delta y(t_i) = y(t_i) - y(t_{i-1}) > 0 \tag{5}$$

2. Abrupt drops in $y(t)$, when compared to the local degradation pattern of neighboring points, are considered outliers unless they are immediately followed by a consistent

degradation trend. In this case, the drop is interpreted as a natural event of accelerated aging rather than an inconsistency. The detection rule is expressed in (6), where $\mu_{\Delta y}$ and $\sigma_{\Delta y}$ are, respectively, the mean and standard deviation of the negative variations in cluster $\mathcal{C}$.

$$\begin{cases} \Delta y(t_i) = y(t_i) - y(t_{i-1}) < \mu_{\Delta y} - 2\sigma_{\Delta y} \\ \Delta y(t_{i+1}) = y(t_{i+1}) - y(t_i) \geq \mu_{\Delta y} - 2\sigma_{\Delta y} \end{cases} \tag{6}$$

This criterion detects outliers as abrupt drops in y_t that significantly deviate from the expected local variation. The 2σ threshold assumes that the distribution of negative variations within each cluster $\mathcal{C}$ is approximately normal. Importantly, the analysis is carried out within clusters so that variability is assessed locally rather than globally.

Furthermore, the second condition in (6) ensures that an abrupt drop is only considered an outlier if it is not immediately followed by a consistent degradation trend. This distinction is crucial to avoid false positives, for example, in cases where the natural degradation of components such as bushings produces sudden but legitimate declines. The values flagged as outliers are replaced by empty cells, preventing them from influencing subsequent analyses. The proposed AD algorithm combines domain-specific assumptions with local statistical criteria, improving the reliability of outlier detection in power transformer performance index data.

At the end, it is important to emphasize that power transformers do not exhibit self-recovery of performance. The cellulosic insulation ages irreversibly through hydrolysis and oxidation, leading to kraft paper depolymerization and a permanent loss of mechanical strength [24,25]. Although interventions like oil drying and acid removal can slow degradation, they cannot reverse the chemical damage that has already occured. The aging process is autocatalytic, accelerated by moisture and acidic by-products, ensuring that performance improvement stems only from corrective maintenance [26]. The degree of polymerization (DP) monotonically declines over service life and can only be restored by replacing the insulating material [27]. The transformer lifetime is consumed cumulatively, and it is particularly influenced by hot-spot temperatures as prescribed in IEC/IEEE loading guides [28]. High hot-spot temperatures degrade the insulation irreversibly and increase brittleness [29,30]. This foundational understanding justifies the developed algorithm's assumption of degrading performance.

2.3. Statistical Validation of Maintenance Interventions

To assess whether a recorded intervention produced a statistically significant improvement in the performance index $y(t)$, a local comparison strategy is applied, which is based on the last observation immediately before the intervention and the first two observations available after it. Let t_0 denote the intervention instant. The last pre-intervention observation is denoted by y_{pre}, while the two post-intervention values are denoted by $y(t_0)$ (if available at the same time as the intervention) and $y(t_{0^+})$ (the first non-intervention observation with $t > t_0$). If no measurement exists exactly at t_0, the first two non-intervention points with $t > t_0$ are used instead.

The differences relative to the baseline are defined in (7). The sample mean $\bar{d}$ and variability s_d of these differences are computed as in (8). The test statistic in (9) follows Student's t distribution under the null hypothesis with df $= 1$ degree of freedom.

$$d_1 = y(t_0) - y_{\text{pre}} \qquad \text{and} \qquad d_2 = y(t_{0^+}) - y_{\text{pre}} \tag{7}$$

$$\bar{d} = \frac{d_1 + d_2}{2} \qquad \text{and} \qquad s_d = \sqrt{(d_1 - \bar{d})^2 + (d_2 - \bar{d})^2} \tag{8}$$

$$t = \frac{\bar{d}}{s_d/\sqrt{2}}, \qquad \mathrm{df} = 1 \tag{9}$$

The hypotheses are formally written as $H_0: \bar{d} \leq 0$ versus $H_1: \bar{d} > 0$. The one-sided p-value is defined as $p = \Pr\{T_1 \geq t\} = \mathrm{sf}(t;1)$ where T_1 is a t random variable with one degree of freedom. Here, $\Pr\{\cdot\}$ denotes probability: that is, $\Pr\{A\}$ is the probability that event A occurs. In addition, the notation $\mathrm{sf}(t;1)$ refers to the survival function of the t distribution with one degree of freedom, defined as $\mathrm{sf}(x) = 1 - F(x) = \Pr(X \geq x)$, where $F(x)$ is the cumulative distribution function (CDF). At the end, the decision rule relies exclusively on the p-value.

- If $p < \alpha$, the intervention is classified as Effective;
- If $p \geq \alpha$, the intervention is classified as Not Statistically Effective (NSE).

2.4. Particle Filters for Predicting the Performance Index

Subsequently, two custom Monte Carlo-based filters developed in this study and referred to as AD-SIS and AD-Bootstrap are applied. Unlike standard Sequential Importance Sampling (SIS) and Bootstrap filters, these frameworks incorporate specific mechanisms to address irregular sampling, autoregressive forecasting, and condition-based classification. Monte Carlo techniques are widely used for probabilistic inference in nonlinear dynamic systems [8,31,32] and constitute an important branch of Artificial Intelligence (AI) for modeling uncertainty.

Initially, the unobserved signal (hidden states) $\mathbf{x}_t$ with $t \in \mathbb{N}$ is considered to be modeled as a Markov process with an initial distribution $p(\mathbf{x}_0)$ and transition probability $p(\mathbf{x}_t \mid \mathbf{x}_{t-1})$. The observations $\mathbf{y}_t$ with $t \in \mathbb{N}^*$ are assumed to be conditionally independent given the stochastic process and the marginal distribution $p(\mathbf{y}_t \mid \mathbf{x}_t)$. Additionally, let $\mathbf{x}_{0:t} \triangleq \{x_0, \ldots, x_t\}$ and $\mathbf{y}_{1:t} \triangleq \{y_1, \ldots, y_t\}$ represent, respectively, the signal and the observations at time t. First, Bayes' theorem is applied to compute $p(\mathbf{x}_t \mid \mathbf{y}_{1:t-1})$ in (10).

$$p(\mathbf{x}_{0:t} \mid \mathbf{y}_{1:t}) = \frac{p(\mathbf{y}_{1:t} \mid \mathbf{x}_{0:t})\, p(\mathbf{x}_{0:t})}{\int p(\mathbf{y}_{1:t} \mid \mathbf{x}_{0:t})\, p(\mathbf{x}_{0:t})\, d\mathbf{x}_{0:t}} \tag{10}$$

In the Sequential Importance Sampling (AD-SIS) filter, the importance sampling method produces an estimate of $p(\mathbf{x}_{0:t} \mid \mathbf{y}_{1:t})$, defined as $\hat{P}_N(d\mathbf{x}_{0:t} \mid \mathbf{y}_{1:t})$, without altering the past simulated trajectories, given by $\mathbf{x}_{0:t-1}^{(i)}$, with $i = 1, \ldots, N$, where N is the number of independent and identically distributed (i.i.d.) random samples, which are referred to as particles [32]. Thus, the importance function $\pi(\mathbf{x}_{0:t} \mid \mathbf{x}_{1:t})$ at time t, understood as a marginal distribution at $t-1$, satisfies the relationship in (11), which is obtained by a recursive structure of the posterior distribution based on the Markov assumption, serving as the foundation for Sequential Importance Sampling. Furthermore, the importance weights $\tilde{w}_t^{(i)}$ are computed recursively, as shown in (12).

$$\pi(\mathbf{x}_{0:t} \mid \mathbf{y}_{1:t}) = p(\mathbf{x}_0) \prod_{k=1}^{t} p(\mathbf{x}_k \mid \mathbf{x}_{k-1}) \tag{11}$$

$$\widetilde{w}_t^{(i)} \propto \widetilde{w}_{t-1}^{(i)} \frac{p\left(\mathbf{y}_t \mid \mathbf{x}_t^{(i)}\right) p\left(\mathbf{x}_t^{(i)} \mid \mathbf{x}_{t-1}^{(i)}\right)}{\pi\left(\mathbf{x}_t^{(i)} \mid \mathbf{x}_{0:t}^{(i)}, \mathbf{y}_{1:t}\right)} \tag{12}$$

In the AD-Bootstrap filter, the importance weights are considered as $p(\mathbf{y}_t \mid \tilde{\mathbf{x}}_t^{(i)})$, where $\tilde{\mathbf{x}}_t^{(i)} \sim p(\mathbf{x}_t \mid \mathbf{x}_{t-1}^{(i)})$. This modification, compared to the AD-SIS filter, enhances the adjustment of particles to observations by eliminating additional importance functions

present in the latter. As a result, the AD-Bootstrap filter discards low-relevance particles and focuses computations on the most representative ones.

The observation $\mathbf{y}_t$ is assumed to be conditionally dependent on the latent state through an observation function $\mathbf{h}_t(\cdot)$, which is also subject to measurement noise. In this study, two forms of observation models were considered:

1. Direct observation with additive Gaussian noise, modeled as $\mathbf{h}_t(\mathbf{x}_t) = \mathbf{x}_t + \boldsymbol{\eta}_t$, with $\boldsymbol{\eta}_t \sim \mathcal{N}(\mathbf{0}, \sigma^2\mathbf{I})$;
2. A likelihood function with exponential form, $\mathcal{L}(\mathbf{x}_t; \mathbf{y}_t) = \exp\left(-\frac{1}{2}\frac{(\mathbf{x}_t - \mathbf{y}_t)^2}{\sigma^2}\right)$, which is suitable for simulating asymmetric or peaked behaviors in the observation process.

The transition model at time t is defined as $\mathbf{x}_t = \text{clip}(f_t(\mathbf{x}_{t-1}) + \boldsymbol{\varepsilon}_t,\ \mathbf{0},\ \mathbf{1}),\quad \boldsymbol{\varepsilon}_t \sim \mathcal{N}(\mathbf{0}, \sigma^2\mathbf{I})$, where $f_t(\cdot)$ is a scalar-valued function applied component-wise to each particle in $\mathbf{x}_{t-1}$, and $\text{clip}(\cdot)$ limits each resulting element to the interval $[0, 1]$, ensuring consistency with the normalized domain of the performance index. The following forms were considered for $f_t(x)$, where x denotes a generic particle in the vector $\mathbf{x}_{t-1}$: sine-based, $f_t(x) = 0.5(1 + \sin(x))$; linear decay, $f_t(x) = 0.8x$; quadratic with sine, $f_t(x) = 0.5(1 + \sin(x)) + 0.1x^2$; and uniform noise, $x_t \sim \mathcal{U}(0, 1)$, independently drawn.

2.5. Filter Performance Metrics

Additionally, to evaluate the performance of the filters, the following metrics are used: MAE (Mean Absolute Error) and R^2 (coefficient of determination), as defined in Equations (13) and (14), respectively. In this context, $\hat{y}_l$ and y_l denote, in that order, the predicted and observed values of the performance index at instance l, while $\overline{y}$ represents the mean of the observed values. High-performance models are expected to exhibit low MAE values, indicating minimal prediction errors, and R^2 values close to one, reflecting the high explanatory power of the model.

$$\text{MAE} = \frac{1}{n}\sum_{l=1}^{n}|\hat{y}_l - y_l| \tag{13}$$

$$R^2 = 1 - \frac{\sum_{l=1}^{n}(y_l - \hat{y}_l)^2}{\sum_{l=1}^{n}(y_l - \overline{y})^2} \tag{14}$$

The best hyperparameter configurations for each model are determined using a composite score, as defined in (15), which combines both prediction accuracy and explanatory power. Lower values of the composite score indicate better overall performance, as they reflect a combination of reduced prediction error (via MAE) and improved goodness of fit (via R^2).

$$\text{Composite score} = \text{MAE} + (1 - R^2) \tag{15}$$

Each particle was initialized by sampling from a uniform prior distribution over the interval $[0, 1]$, which corresponds to the normalized domain of the performance index. The state transition model incorporated Gaussian noise added to each particle with the standard deviation σ. In Monte Carlo methods, the typical estimation error decreases on the order of $\mathcal{O}(1/\sqrt{N})$ as the number of samples N increases [33,34] yet with diminishing returns beyond a certain threshold. The set $N \in \{400; 800; 1000; 1600; 4000; 10{,}000\}$ was selected to span a wide computational range that enables an evaluation of the error curve as a function of N, where precision gains stabilize, typically between approximately 10^3 and a few thousand particles [35]. It is also useful to observe convergence behavior and compare outcomes to a high asymptotic reference point, $N = 10{,}000$.

Adaptive resampling via the Bootstrap approach is triggered when the Effective Sample Size (ESS) falls below $N/2$. This is a well-established heuristic widely reported in the literature [36,37], which helps prevent weight degeneracy while preserving particle diversity. For the process and observation noise, the levels were set to $\sigma \in \{0.005, 0.01, 0.05, 1.5, 2.0\}$, with all values defined over the normalized domain $[0, 1]$, as follows [38]:

- Low values of σ (0.005 to 0.01): represent near-deterministic dynamics where weight collapse is likely if the likelihood function is sharp.
- Intermediate value (around 0.05): corresponds to typical post-normalization variability, offering a balance between tracking flexibility and smoothing.
- High values (1.5 to 2.0): serve as stress tests (negative controls), inducing excess diffusion that challenges the filter's robustness under over-smoothed or poorly identifiable regimes.

2.6. Workflow of the Developed Method

For better visualization, the developed method is outlined in the flowchart of Figure 1. It depicts the main sequence of steps described in Section 2, which comprise the designed approach, from data input to output.

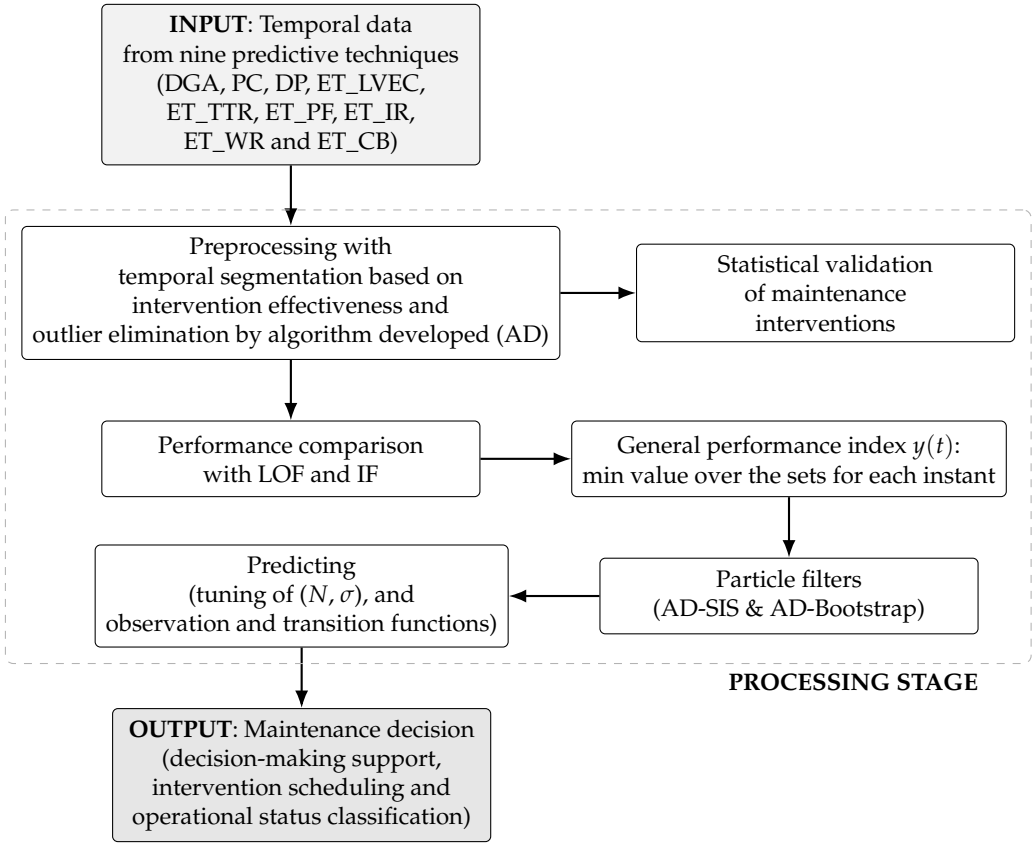

Figure 1. Workflow of the methodology developed in this study.

As illustrated, the workflow in Figure 1 presents the sequential logic of the method, from data preprocessing to decision-making support, and provides a basis for the reader to follow the subsequent results.

3. Results and Discussion

3.1. Operating Conditions, Weather Events and Maintenance Interventions

In this study, the simulated faults, defined according to the operating conditions of each unit, and their respective implications for the predictive techniques are presented in Table 2. To enhance comparability and emphasize the observed effects, five power transformers (TR1 to TR5) immersed in insulating mineral oil with broadly similar characteristics were selected.

Table 2. Power transformers: simulated operating conditions, weather events, maintenance interventions, and observed effects.

Equipment	Operating Conditions, Weather Events and Maintenance Interventions	Observed Effects
TR1	• Natural aging. • No electrical overloads. • No severe atmospheric events or weather conditions. • No damaging systemic transients. • No maintenance intervention.	Slight and general decay in the performance indices of various techniques.
TR2	• Natural aging. • No electrical overloads. • No severe atmospheric events or weather conditions. • No damaging systemic transients. • No maintenance interventions.	Slight and general decay in the performance indices of various techniques.
TR3	• With electrical overloads. • Without severe atmospheric events and bad weather. • Without damaging systemic transients. • With maintenance interventions.	Accelerated decay in the performance indices of DGA, DP, and a slightly lower decay in ET_IR, ET_PF, and PC.
TR4	• Normal loading. • With severe atmospheric events. • With severe weather conditions and water penetration through the seals in the active part. • With systemic transients that are stressful to the insulation. • With maintenance interventions and bushing replacement.	Accelerated decay in the performance indices of PC, ET_IR, ET_PF, and ET_CB, with a slightly lower decay in DGA and DP.
TR5	• With electrical overloads in some years and not in others. • No severe atmospheric events and bad weather. • No stressful systemic transients. • With maintenance interventions.	Accelerated decay in the performance indices of DGA and DP with a slightly faster decay in ET_IR and PC.

Table 2 includes the adoption of a common set of predictive techniques and uniform data-sampling procedures, which collectively provide a standardized framework for performance assessment. While the equipment shares these structural and methodological attributes, it differs in specific operational aspects, such as the occurrence of electrical

overloading, exposure to extreme weather events, and the execution of maintenance interventions. These controlled variations allow for a comparative analysis of how distinct fault scenarios influence the outcomes of the predictive techniques.

Although the operating conditions and fault scenarios presented in Table 2 are simulated, they were designed to reproduce patterns actually found in practice. Each case mirrors plausible degradation processes and intervention outcomes, showing how stress factors such as overloading, weather events, and maintenance actions interact with the deterioration of insulating materials and structural components. By integrating a broad range of predictive techniques, the dataset preserves completeness and represents consistent behaviors across different scenarios. Hence, this synthetic yet realistic construction ensures methodological control while still reflecting field-relevant dynamics, thus strengthening the connection between simulated analysis and operational evidence.

3.2. Performance Comparison Between Artificial Intelligence Algorithms Tested and the One Developed

Tables 3 and 4 present the comparison of the success rates of the outlier classification, based on the labeling provided by experts in power transformer maintenance, considering the three algorithms evaluated: the Local Outlier Factor (LOF), Isolation Forest (IF) and the algorithm designed (AD) in this work.

Table 3. Success rates of the applied tools for TR1 to TR3.

Predictive	**TR1**			**TR2**			**TR3**		
Technique	**LOF**	**IF**	**AD**	**LOF**	**IF**	**AD**	**LOF**	**IF**	**AD**
DGA	100%	80.0%	100%	100%	80.0%	100%	100%	84.1%	100%
PC	100%	85.7%	100%	98.3%	82.0%	97.1%	98.3%	84.1%	100%
DP	100%	80.0%	100%	100%	80.0%	100%	100%	87.4%	100%
ET_LVEC	94.3%	91.4%	100%	94.3%	91.4%	100%	94.3%	91.4%	100%
ET_PF	100%	82.9%	97.1%	98.3%	85.3%	100%	98.3%	87.4%	91.4%
ET_TTR	97.1%	94.3%	94.3%	97.1%	94.3%	94.3%	97.1%	94.3%	94.3%
ET_IR	100%	85.7%	97.1%	98.3%	85.3%	91.4%	98.3%	87.4%	97.1%
ET_WR	94.3%	88.6%	91.4%	94.3%	88.6%	100%	94.3%	88.6%	91.4%
ET_CB	100%	82.9%	94.3%	100%	88.5%	100%	100%	88.5%	100%
Result	98.4%	85.7%	97.1%	97.8%	86.2%	98.1%	97.8%	88.1%	97.1%

Table 4. Success rates of the applied tools for TR4 and TR5.

Predictive	**TR4**			**TR5**		
Technique	**LOF**	**IF**	**AD**	**LOF**	**IF**	**AD**
DGA	94.3%	94.3%	97.1%	91.7%	81.7%	91.4%
PC	94.3%	94.3%	100%	93.8%	89.2%	91.4%
DP	97.1%	91.4%	97.1%	100%	91.4%	97.1%
ET_LVEC	94.3%	91.4%	91.4%	94.3%	91.4%	100%
ET_PF	88.6%	85.7%	100%	100%	84.5%	97.1%
ET_TTR	97.1%	94.3%	94.3%	97.1%	94.3%	94.3%
ET_IR	82.9%	85.7%	100%	100%	87.5%	82.9%
ET_WR	94.3%	88.6%	91.4%	94.3%	88.5%	97.1%
ET_CB	95.6%	83.1%	100%	100%	82.9%	100%
Result	93.2%	89.9%	96.8%	96.8%	87.9%	94.6%

For the LOF, the main hyperparameter is the number of nearest neighbors k, which controls the local density estimation. To determine the optimal value of k for each temporal cluster in the LOF, the Silhouette score (S) was employed, defined in (16) [21,39,40], where

a_i denotes the mean intra-cluster distance, b_i represents the mean nearest-cluster distance, and n is the number of samples in the cluster, as illustrated in Figure 2.

$$S = \frac{1}{n} \sum_{i=1}^{n} \frac{b_i - a_i}{\max(a_i, b_i)} \tag{16}$$

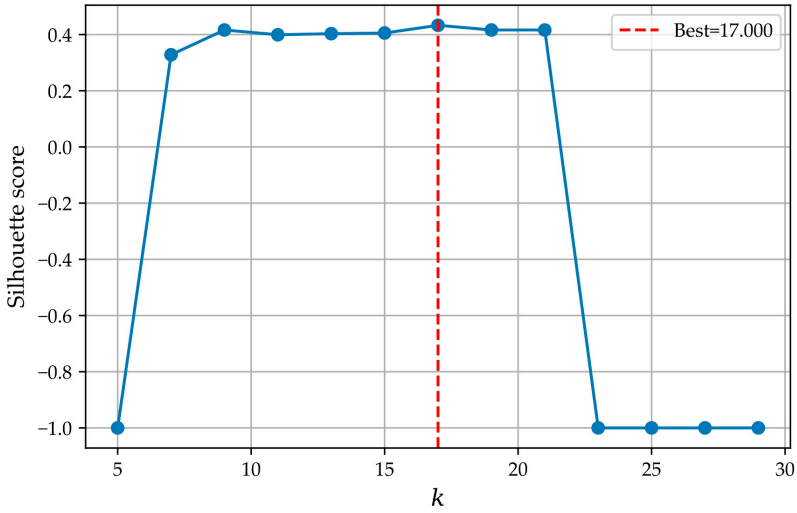

Figure 2. Example of Silhouette curve for a cluster of the predictive technique ET_PF, which is used to determine the optimal k of the LOF for TR4.

Similarly, for the IF, the contamination parameter, which represents the expected proportion of outliers in Scikit-learn library [41–43], was optimized using a grid: contamination $\in \{0.01, 0.03, 0.05, \ldots, 0.20\}$, because the lower bound reflects the realistic assumption that anomalies in equipment time series are rare, while the upper bound accounts for clusters with higher proportions of abnormal behavior due to concentrated interventions. Figure 3 exemplifies that optimization process.

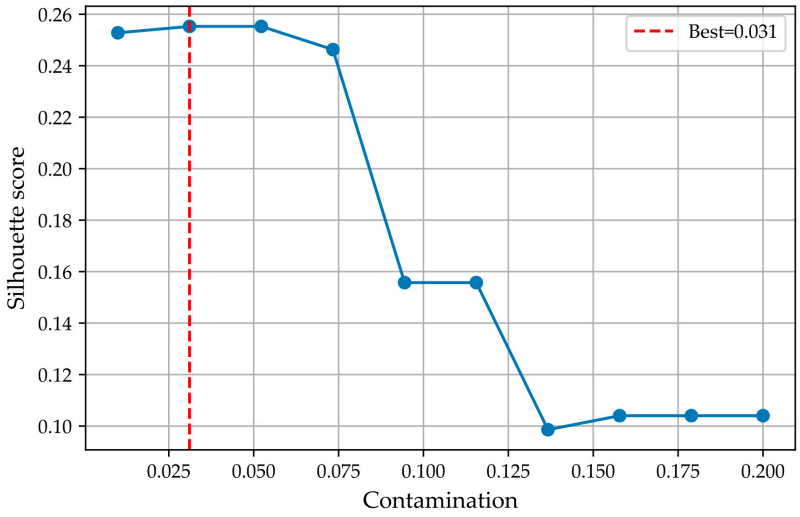

Figure 3. Example of Silhouette curve for a cluster of the predictive technique ET_TTR, which is used to determine the optimal contamination of the IF for TR4.

The results presented in Tables 3 and 4 highlight the high success rate of the proposed algorithm (AD). For instance, in the DGA, PC, and DP techniques, AD achieved a success rate of 100% for TR1 and TR3, whereas the LOF and IF almost always exhibited lower

performances. On average, considering the five evaluated transformers, AD reached a success rate of 96.7%, which is superior to IF (87.6%) and comparable to the LOF (96.8%). It is worth noting that IF consistently yielded lower accuracies among the tested methods, although still maintaining values above 80%. These findings demonstrate that the proposed strategy is consistent across different techniques and power transformers, confirming its robustness and broad applicability.

3.3. Hyperparameters of the Particle Filters

Tables 5 and 6 summarize the optimal hyperparameter configurations identified for each particle filter and power transformer based on training performance, corresponding to AD-SIS and AD-Bootstrap, respectively. A time-aware split was adopted, where the first 70% of the temporal data was allocated to the training set and the subsequent 30% to the testing set, in order to avoid data leakage and maintain the natural sequence of events.

Table 5. Best hyperparameter configuration based on training performance for each power transformer (AD-SIS).

Equipment	Transition	Observation	N	σ
TR1	Uniform	Exponential	1000	0.01
TR2	Uniform	Gaussian	800	0.01
TR3	Uniform	Exponential	4000	0.005
TR4	Uniform	Exponential	4000	0.005
TR5	Uniform	Exponential	400	0.005

Table 6. Best hyperparameter configuration based on training performance for each power transformer (AD-Bootstrap).

Equipment	Transition	Observation	N	σ
TR1	Uniform	Exponential	10,000	0.005
TR2	Uniform	Exponential	10,000	0.01
TR3	Uniform	Exponential	10,000	0.005
TR4	Uniform	Exponential	10,000	0.005
TR5	Uniform	Exponential	10,000	0.005

All reported results were obtained using the best-ranked combinations of transition and observation functions, as determined by the consolidated analysis. For the AD-Bootstrap filter, increasing the number of particles to $N = 10{,}000$ consistently resulted in outstanding predictive performance. The test set R^2 values approached unity, reaching 0.99998, 0.99988, 0.99999, 0.99998, and 0.99999 for TR1 through TR5, respectively. Furthermore, the training metrics exhibited extremely low error levels with MAE values ranging from 0.00033 to 0.00037. These findings demonstrate the model's strong ability to fit the training data while maintaining excellent generalization when a sufficiently high number of particles is used.

These results provide an intuitive understanding of how the number of particles (N) and the noise level (σ) jointly influence filter performance. For instance, for transformer TR1, the best configuration for the AD-Bootstrap filter was $N = 10{,}000$ and $\sigma = 0.005$, using a uniform transition function and an exponential observation function. This same combination yielded the best result on the test set. In the case of the AD-SIS filter, the optimal configuration on both the training and test sets was $N = 1000$ and $\sigma = 0.01$, under the same transition and observation functions as AD-Bootstrap. Figures 4 and 5 present the composite score heatmaps for the test set of TR1 under the evaluated configurations of AD-Bootstrap and AD-SIS filters with the best-performing combination of transition and observation functions.

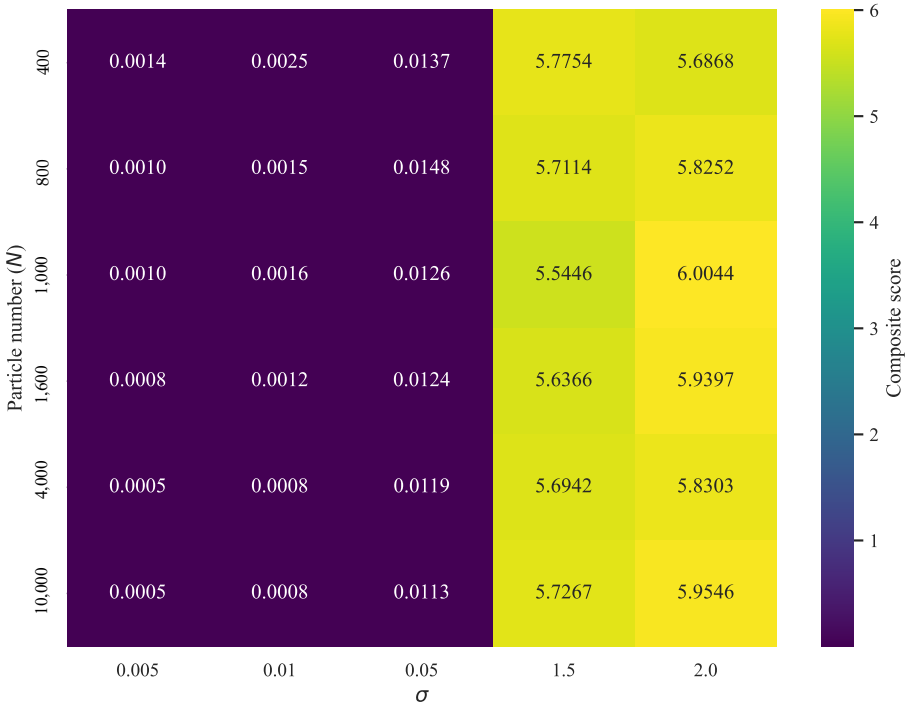

Figure 4. Composite score heatmap for TR1 test set, AD-Bootstrap, uniform transition, and exponential observation.

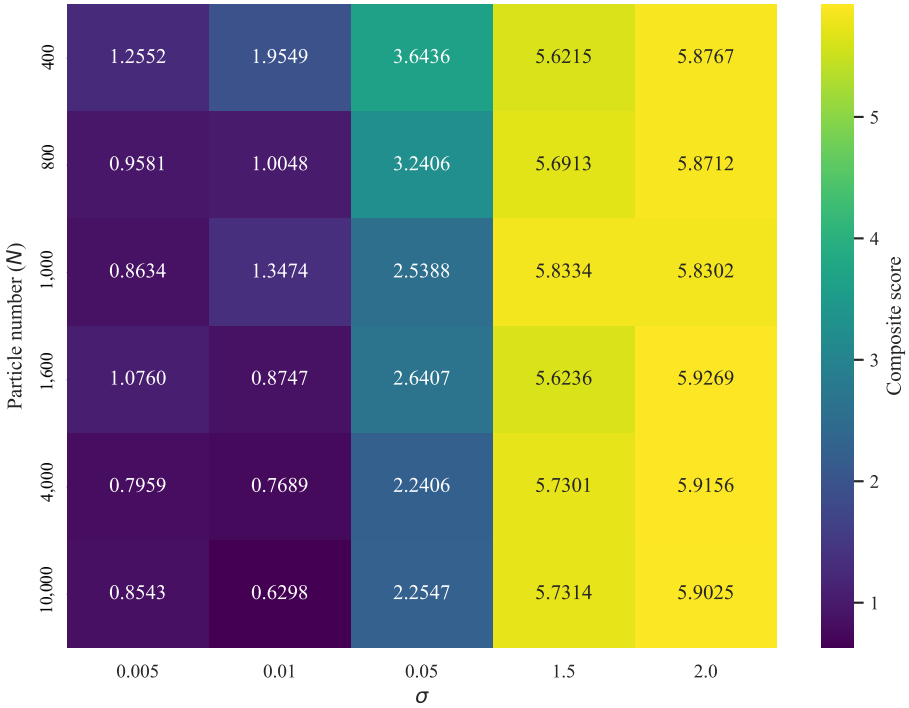

Figure 5. Composite score heatmap for TR1 test set, AD-SIS, uniform transition, and exponential observation.

Conversely, the Sequential Importance Sampling (AD-SIS) filter exhibited substantially lower predictive accuracy even when using its best configuration of transition and observation functions. The best R^2 values on the test set were significantly lower, with some even negative (e.g., 0.4430 for TR1, −0.3060 for TR2, and −1.6606 for TR4), and only moderate or acceptable results for TR3 (0.5678) and TR5 (0.2601). Although a few

configurations achieved decent training performance (with MAE ranging from 0.0618 to 0.0816), the large gap between training and testing metrics indicates overfitting and limited generalization capacity. These outcomes suggest that AD-SIS is more sensitive to noise and less robust than AD-Bootstrap, especially when using fewer particles or under conditions of higher model variance.

3.4. Execution Time Analysis and Memory Usage

The computational time required by each configuration was evaluated as a function of the number of particles N. All simulations were executed on a laptop equipped with an Intel(R) Core(TM) i5-1035G1 CPU @ 1.0–1.2 GHz (8 logical cores) and 12 GB of RAM, running Windows 11 Home 64-bit. The implementation was developed in Python 3.12 using the Spyder IDE. Figures 6 and 7 illustrate, for TR1, the computational runtime (in seconds) of the particle filters as a function of the number of particles (N) for different noise levels (σ). Each curve represents the mean runtime across transition and observation models, including both training and test phases.

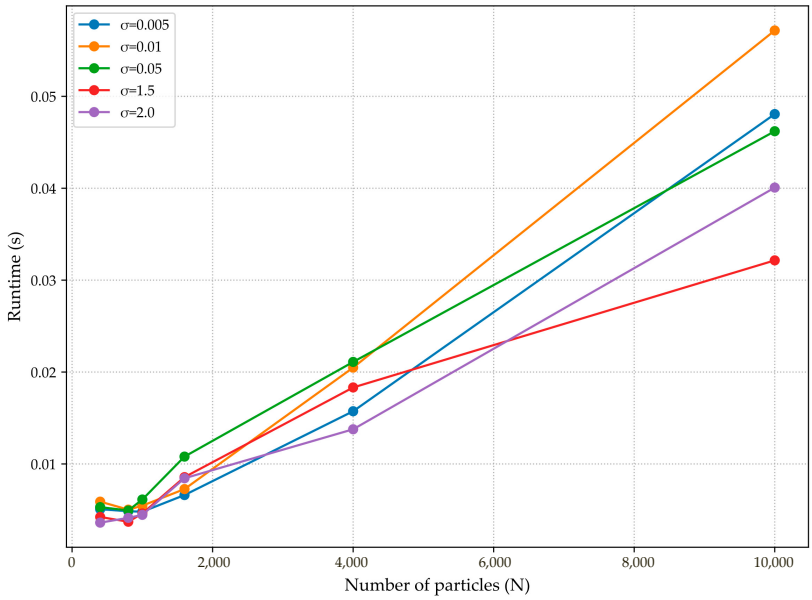

Figure 6. Runtime as a function of the number of particles (N) for different noise levels (σ) in TR1, averaged across transition and observation models, including both training and test phases for the AD-Bootstrap filter.

The runtime in Figures 6 and 7 increases approximately linearly with N for all levels of σ, reflecting the additional sampling and weight update operations required by particle filters. This analysis is essential to assess the practical feasibility of the proposed models, since although larger N values generally improve accuracy, as illustrated in Figures 4 and 5, the execution cost must remain acceptable for real-world applications. Moreover, it is necessary to seek a balance between computational cost and the improvement in the composite score given in (15), as beyond a certain point the accuracy gains become marginal relative to the additional runtime.

In addition, the computational assessment considered both runtime and memory usage, since these aspects are decisive for the feasibility of particle filter implementations. In that way, peak memory was measured with *tracemalloc* to capture Python-level allocations. Although native buffers (such as those handled by NumPy) may not be fully accounted for, the observed memory footprints remained well below the RAM capacity of a standard laptop. While the full set of results was obtained across all (N, σ) configurations, Table 7

highlights both the maximum and minimum runtime and memory usage observed per transformer and filter. This representation not only indicates the upper bound of execution time but also makes explicit the associated peak memory usage. It is interesting to note that since the series lengths across TR1 to TR5 are similar, the most critical runtime and memory usage values are essentially the same for all transformers, being driven primarily by the (N, σ) configuration rather than by equipment-specific characteristics.

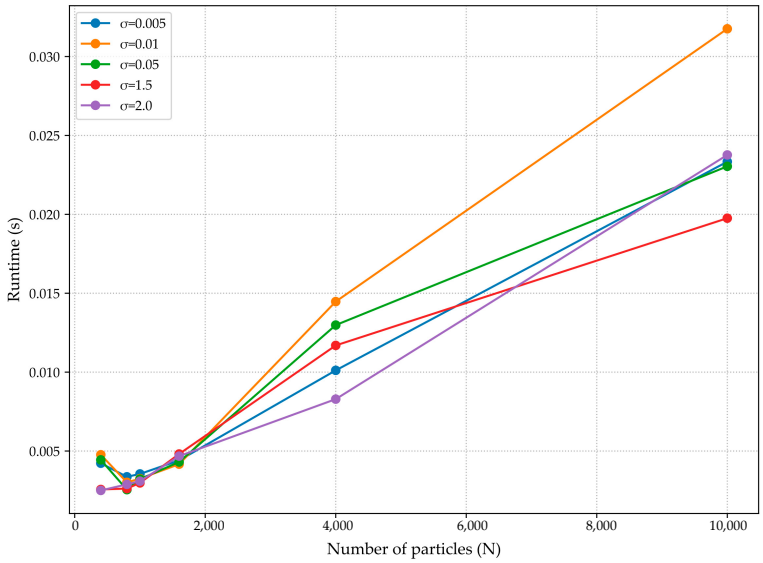

Figure 7. Runtime as a function of the number of particles (N) for different noise levels (σ) in TR1, averaged across transition and observation models, including both training and test phases for the AD-SIS filter.

Table 7. Runtime and peak memory from TR1 to TR5: AD-Bootstrap versus AD-SIS across N and σ.

Configuration	Average Runtime (s)	Peak Memory (MB)	Filter
$N = 400, \sigma = 0.005$	0.01	0.02	AD-Bootstrap
$N = 10{,}000, \sigma = 2.000$	0.04	0.51	AD-Bootstrap
$N = 400, \sigma = 0.005$	0.01	0.02	AD-SIS
$N = 10{,}000, \sigma = 2.000$	0.02	0.46	AD-SIS

The results in Table 7 show that memory usage remained very modest across all settings, even for $N = 10{,}000$ particles. Thus, runtime is the dominant limiting factor in practice, whereas memory requirements are not expected to restrict real-world applications on standard hardware. The relative difference between AD-Bootstrap and AD-SIS mainly reflects the resampling overhead of the former, confirming that the performance gain of AD-Bootstrap comes at the cost of longer execution times but without substantial memory impact.

3.5. Future Behavior Simulation and Technical Assessment of Equipment Operational Patterns

To simulate the future behavior of the equipment performance index, a forecasting strategy based on the AD-Bootstrap particle filter was employed, using the best configuration identified during the training phase for each transformer. This configuration includes the best combination of transition and observation models, particle count N, and noise level σ. In the absence of actual future observations, the forecast was conducted under a conservative hypothesis: no new maintenance actions are performed, and the system undergoes continuous natural degradation. This assumption reflects a worst-case scenario, which is relevant to planning and risk analysis in asset management.

At each forecasting step, the most recent estimated value is reused as a proxy observation to feed the filter, forming an autoregressive process. This iterative procedure allows the uncertainty to propagate throughout the horizon, generating a sequence of performance index estimates. To ensure that the resulting trajectory remains physically consistent, i.e., exhibits progressive degradation, a controlled correction mechanism is applied. The procedure includes the following:

1. Trend correction: At each step, the local trend is estimated by fitting a linear model to the last k predicted values. If the trend is positive (indicating improvement), it is replaced by a fixed negative slope to ensure a conservative decay pattern.
2. Noise injection: A small Gaussian perturbation is added at every iteration to simulate the intrinsic variability of equipment behavior, accounting for minor fluctuations that may arise even in the absence of external events.
3. Value clipping: All predicted values are constrained to the interval $[0, 1]$ to maintain consistency with the normalized domain of the performance index.

This approach avoids unrealistic increases in the performance index when no maintenance is performed and results in a smooth downward curve that represents the system's natural aging. The forecasted values offer a practical basis for estimating degradation timelines and scheduling preventive interventions. Figure 8 illustrates the predicted decline in the performance index of transformer TR1 under ideal operating conditions with no electrical overloads, nor severe weather events, nor harmful transients, nor maintenance actions.

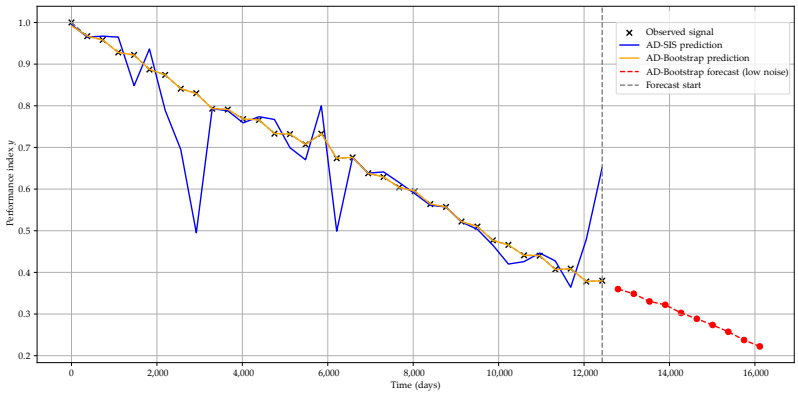

Figure 8. Predictive modeling of performance index dynamics for TR1 via AD-Bootstrap and AD-SIS filters.

According to the simulation, TR1 is expected to reach a performance index of 0.65 pu (Classification C—Marginal) in approximately 6946 days (around 19 years), and 0.5 pu (Classification D—Poor) in around 9864 days (around 27 years), which significantly increases the probability of failure. These results suggest that timely preventive maintenance could considerably extend the useful life of the equipment.

In the forecast for TR2, this observation is imposed, as depicted in Figure 9, which illustrates the natural degradation trajectory of the performance index y under favorable operating conditions with no electrical overloads, nor atmospheric discharges, nor severe weather events, nor damaging transients in the power system.

Differently from TR1, however, TR2 underwent three maintenance interventions. The first was performed at 3295 days of operation (approximately 9 years), but it proved ineffective, resulting in virtually no change in the performance index. The second intervention, conducted at 7306 days (around 20 years), led to a more substantial improvement, increasing the index from 0.638 pu (Classification C—Marginal) to 0.796 pu (Classification B—Good). Finally, the third intervention, carried out at 11,326 days

of operation (approximately 31 years), raised the performance index from 0.611 pu (Classification C—Marginal) to 0.676 pu (Classification B—Good). This contrast underscores the importance of technically sound maintenance actions in achieving measurable improvements in transformer performance.

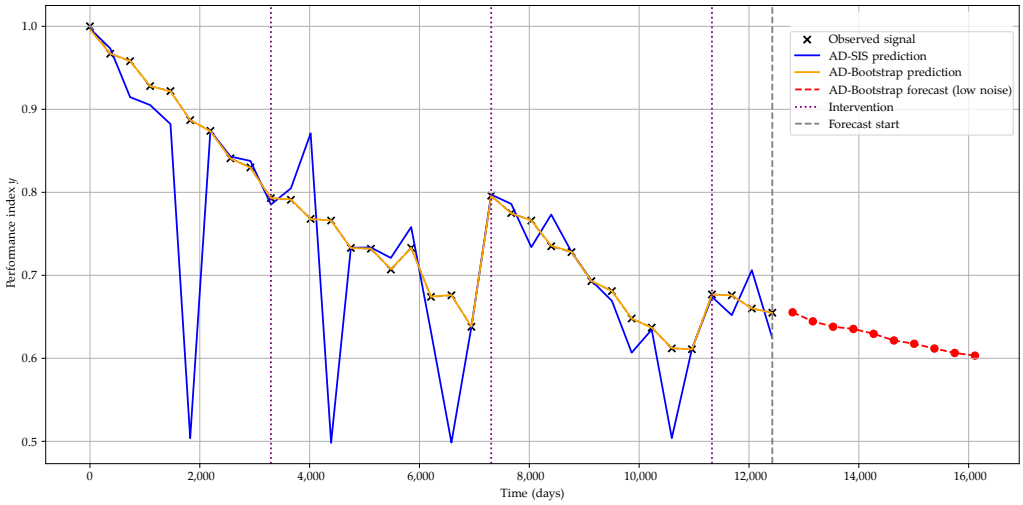

Figure 9. Predictive modeling of performance index dynamics for TR2 via AD-Bootstrap and AD-SIS filters.

Nevertheless, it is important to highlight that as a result of the three maintenance interventions, the forecasting framework developed in this study, when applied via the AD-Bootstrap particle filter, projects that the overall performance index for TR2 will remain above 0.6 pu (Classification C—Marginal) until approximately 16,000 days of operation (around 44 years), which is the upper bound of the forecasting window. This projected trajectory reflects a considerably more favorable degradation profile when compared to TR1. Therefore, the findings strongly support the conclusion that timely and technically appropriate maintenance actions have a substantial positive impact on extending the service life of power transformers, as quantitatively captured by the developed methodology.

In that way, Figure 10 presents the degradation trajectory of the overall performance index for TR3 under adverse operating conditions. The equipment was subjected to electrical overloads, but neither atmospheric events nor severe weather nor harmful system transients occurred. Maintenance interventions were performed. The first intervention occurred at 3295 days of operation (approximately 9 years), and the second occurred at 7306 days (approximately 20 years), during which the overall index showed only a slight improvement from 0.629 pu (Classification C—Marginal) to 0.693 pu (Classification B—Good).

This limited recovery is explained by the fact that although the oil treatment improved the performance indices of the Physicochemical Tests (PC), Insulation Resistance (ET_IR), and Power Factor (ET_PF), the Degree of Polymerization (DP) was significantly impacted by the electrical overloads. These overloads accelerated the degradation of the cellulose insulation in the windings, which was a component directly associated with DP measurements. When comparing Figure 10 (TR3) with Figure 9 (TR2), it becomes evident that TR3 undergoes faster degradation due to the effects of overload. Notably, the third intervention carried out on TR3 at 10,595 days (around 29 years) proved ineffective, as no significant improvement in the overall performance index was observed following its execution. In such scenarios, the tool developed in this study proves valuable for predicting the equipment's degradation trend, enabling preventive maintenance actions or even its removal from operation at a more favorable time.

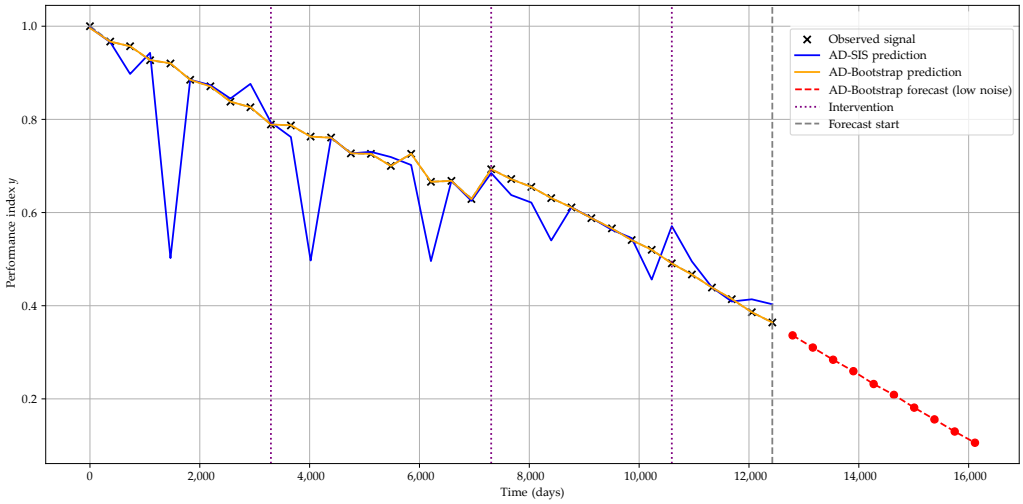

Figure 10. Predictive modeling of performance index dynamics for TR3 via AD-Bootstrap and AD-SIS filters.

The evolution of the performance index y for TR4 reveals the impact of various stressors encountered throughout its operational life, as illustrated in Figure 11.

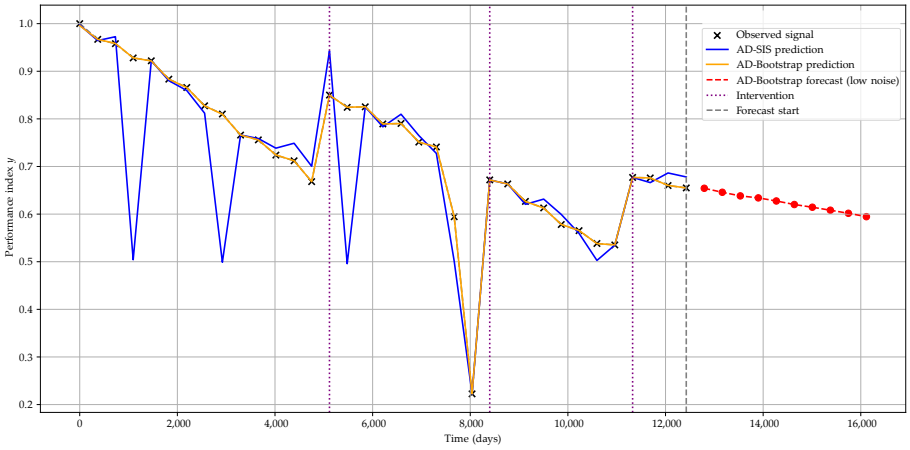

Figure 11. Predictive modeling of performance index dynamics for TR4 via AD-Bootstrap and AD-SIS filters.

Although the transformer operated under nominal loading conditions, it was exposed to a combination of external aggressions, including atmospheric discharges, severe weather events, water ingress through sealing points, and harmful transients in the electrical network. These adverse conditions triggered two maintenance interventions; the second involved the replacement of bushings.

The first intervention, performed at 5116 days of operation (approximately 14 years), resulted in a notable performance improvement, increasing y from 0.67 pu (Classification B—Good) to 0.85 pu (Classification A—Excellent). The second occurred at 8399 days (approximately 23 years), following an abrupt decline in the bushing performance index to 0.22 (Classification E—Very Poor), which was caused by damage attributed to systemic transients. In response, the bushings were replaced preventively prior to catastrophic failure, and additional preventive maintenance actions were carried out on the transformer. As a result, the global performance index recovered to 0.67 (Classification B—Good).

In light of these interventions, the forecasting tool developed in this study, using the AD-Bootstrap particle filter, estimates that the overall performance index will remain close to 0.6 pu (Classification C—Marginal) until approximately 16,000 days of operation

(around 44 years), which is the upper limit of the forecasting window. This outcome reinforces the model's ability to capture long-term trends and highlights the effectiveness of condition-based maintenance strategies in preserving asset performance and extending its operational lifespan.

A similar analysis applies to TR5, whose performance trajectory is depicted in Figure 12. Throughout its operational life, the transformer experienced alternating periods with and without electrical overloads but remained unaffected by atmospheric discharges, severe weather events, and systemic transients, which are factors that typically impose additional stress on insulation systems.

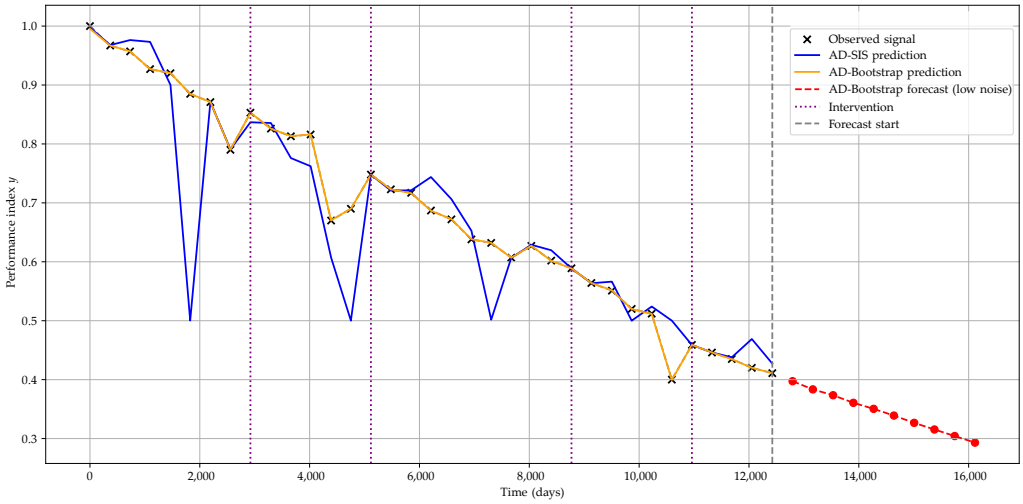

Figure 12. Predictive modeling of performance index dynamics for TR5 via AD-Bootstrap and AD-SIS filters.

Nonetheless, the persistent exposure to overload conditions led to a progressive decline in the overall performance index. In response, four maintenance interventions were executed at 2922 days (approximately 8 years), 5116 days (around 14 years), 8768 days (around 24 years), and 10,961 days (around 30 years). Despite improvements in oil quality parameters following these interventions, their impact on the overall condition of the transformer was limited. The primary reason lies in the accelerated degradation of the cellulose insulation, which was particularly evidenced by the persistent deterioration in the Degree of Polymerization (DP) index. Given that such degradation is irreversible without complete factory-level reconditioning of the windings, the interventions failed to produce sustained improvements in the equipment's health.

This case underscores the value of the predictive framework developed in this study. By revealing consistent long-term downward trends in the general performance index, the tool enables the early identification of irreversible degradation processes and offers quantitative support for asset retirement decisions, thereby contributing to more reliable and cost-effective fleet management strategies.

3.6. Statistical Validation of Maintenance Interventions

Table 8 presents the results of the statistical validation procedure of maintenance interventions for each equipment unit (from TR1 to TR5), considering a significance level of $\alpha = 0.10$. It details, step by step, each parameter employed, as well as the results of Student's t-test and the corresponding p-value. Based on the formulated hypothesis test, the applied maintenance intervention is classified as Effective or Not Statistically Effective (NSE).

The formulation shown in Table 8 formalizes the graphical interpretation of the intervention effectiveness analysis. Thus, what could previously only be visually inferred from the behavior of the performance index after the intervention is now supported by a parametric hypothesis test. Therefore, it was possible to demonstrate, in a mathematical and reproducible manner, whether the variation observed in the performance index after each intervention can be attributed to a real maintenance effect or merely to chance. It is important to highlight, in this sense, that the graphical interpretations are consistent with the statistical results obtained, reinforcing the validity and reliability of the proposed procedure.

Table 8. Results of one-sided predictive t-tests for maintenance interventions using $\alpha = 0.1$.

Equipment	t_0 (Days)	$y(t_0)$	y_{pre}	$y(t_{0^+})$	t-Student	p-Value	Decision
TR1	—	—	—	—	—	—	No intervention
TR2	3295	0.791	0.830	0.768	−4.391	0.929	NSE *
	7306	0.775	0.638	0.766	29.444	0.011	Effective
	11,326	0.676	0.611	0.660	7.125	0.044	Effective
TR3	3295	0.787	0.826	0.763	−4.250	0.926	NSE *
	7306	0.672	0.629	0.655	4.059	0.077	Effective
	10,595	0.467	0.52	0.439	−4.786	0.934	NSE *
TR4	5116	0.824	0.668	0.825	277.133	0.001	Effective
	8399	0.663	0.222	0.627	23.066	0.014	Effective
	11,326	0.676	0.535	0.660	16.595	0.019	Effective
TR5	2922	0.826	0.790	0.813	4.538	0.069	Effective
	5116	0.723	0.69	0.717	10.000	0.032	Effective
	8768	0.564	0.602	0.551	−6.846	0.954	NSE *
	10,961	0.446	0.400	0.435	7.364	0.043	Effective

* The term NSE means Not Statistically Effective.

3.7. Time Series Cross-Validation with One-Step-Ahead Forecasting

The evaluation of the predictive performance of particle filters was conducted to avoid bias from a single train–test split. To this end, a nested temporal cross-validation procedure with one-step-ahead prediction was adopted. In the outer loop, each series was divided into $k = 5$ progressive folds. Moreover, within each training segment, an inner loop ($k = 3$ folds) was applied to select the best hyperparameter configuration (number of particles N, noise level σ, and transition and observation models). This design ensured that model selection was carried out solely on the training data, while the external test fold remained completely unseen until the final evaluation.

The metric used for hyperparameter selection is defined in (15), where lower values indicate a better trade-off between accuracy and explanatory power. Once the best configuration was identified in the inner loop, it was fixed and evaluated on the corresponding test fold. In addition to regression-based indicators, categorical performance was assessed by discretizing the performance index into classes A to E, according to Table 1. The following classification metrics were considered:

1. Strict accuracy (A_{cc}), corresponding to exact matches between predicted and observed classes;
2. Accuracy ± 1 ($A_{cc\pm 1}$), which allows deviations of at most one adjacent class.

Figure 13 summarizes the one-step-ahead nested CV results. Random seeds were deterministically varied across outer/inner folds and candidate configurations (offsets of a base seed) to reduce sensitivity to stochastic sampling and resampling.

The average performance of the AD-Bootstrap and AD-SIS filters, shown in Figure 13, considers all time series evaluated under the nested time-series cross-validation scheme.

The AD-Bootstrap filter achieved globally superior results compared to AD-SIS with a strict accuracy of 85.33% and perfect accuracy ± 1 ($A_{cc\pm 1} = 100\%$). This indicates that even when AD-Bootstrap misclassifies, it tends to remain within the neighborhood of the correct class.

In contrast, AD-SIS exhibited lower values across all metrics with strict accuracy of 79.67% and tolerant accuracy of 97.00%. These findings highlight the superior predictive performance of AD-Bootstrap over AD-SIS in one-step-ahead forecasting scenarios, although the latter still demonstrates reasonable generalization, making it a viable option in contexts where lower computational cost or model simplicity are decisive factors.

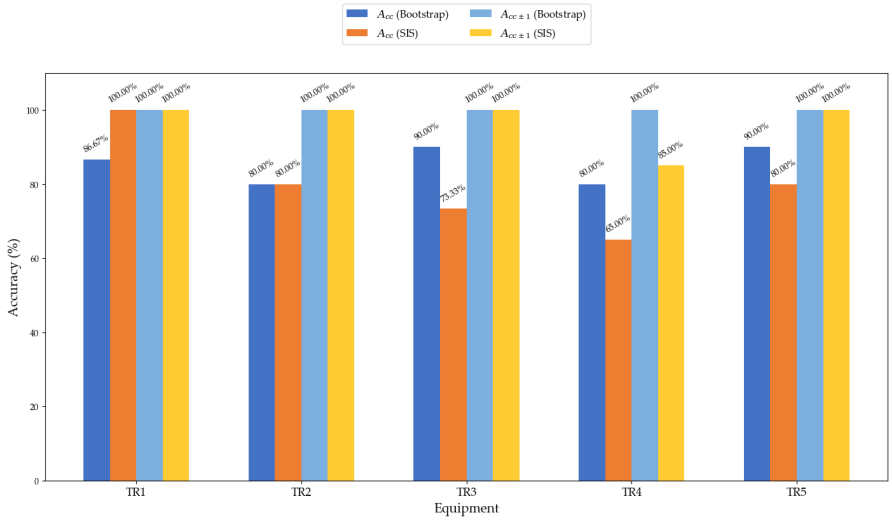

Figure 13. Accuracy comparison between AD-Bootstrap and AD-SIS across power transformers.

Overall, these results demonstrate that particle filters are effective in preserving the ordinal structure of transformer performance classes even under different operating conditions. In particular, the robustness of AD-Bootstrap makes it the most promising candidate for practical deployment.

3.8. Comparison with State-of-the-Art Methods

To perform systematic and comprehensive diagnostics, AI has been employed in the interpretation of DGA. Applications of Multilayer Perceptron networks trained with Levenberg–Marquardt and adaptive backpropagation achieved accuracies above 96% for C_2H_2 and 87% for H_2, significantly outperforming conventional IEEE/IEC methods (key gas and Rogers) [44]. There are also models of autoassociative neural networks combined with Mean Shift, enabling unsupervised diagnostics with accuracies close to 84% [45]. Other AI approaches combine artificial neural networks with rule-based logic, reaching more than 95% accuracy in critical faults [46]. Advances include Double-Stacked Autoencoders, which achieved 96.83% accuracy [47]. Also, a mathematical approach and Support Vector Machines (SVMs) were employed as decision-making methods in hybrid fault diagnosis systems. Tests conducted with 317 real fault datasets from power transformers demonstrated an accuracy of 95.58% for the mathematical approach and 96.23% for the SVM-based model [48]. These contributions highlight that modern AI techniques can outperform traditional diagnostic methods but still present high computational complexity and sensitivity to hyperparameters.

Regarding the aging of cellulosic insulation, AI-based approaches have been applied to diagnostics using the degree of polymerization (DP). For example, temporal networks are explored, where LSTM achieved 92.3% accuracy, outperforming convulotional networks (89.6%) [49]. Despite promising results, these techniques require large volumes of labeled data and high computational costs. Physicochemical tests have also been interpreted with

AI. Hybrid artificial neural networks have been applied, reaching a maximum accuracy of 89% in multiclass classification, although with low interpretability and dependence on input normalization [50]. However, these approaches still depend on limited datasets restricted to specific voltage classes.

Partial discharge (PD) detection by acoustic emission has also benefited from AI. Fourier and wavelet transforms integrated with classification models achieved up to 94% accuracy in controlled conditions [51]. Methods such as Cubic-Support Vector Machine and tree ensembles with bagging surpassed 98% accuracy [52]. Nevertheless, challenges remain, including class imbalance and dependency on the quality of acoustic signals. In addition, the recent production has explored the use of systems analysis and virtual modeling to support predictive maintenance in complex energy infrastructures [53].

In the specific problem addressed in this study (one-step-ahead forecasting of a continuous index mapped into ordinal classes A to E), the AD-Bootstrap filter achieved 85.33% strict accuracy and 100% ± 1-class accuracy, while AD-SIS achieved 79.67% and 97.00%, respectively. Although this is not a direct comparison with other studies, given the differences in datasets, diagnostic and prognostic objectives, and performance metrics, the results obtained here indicate that AD-Bootstrap, in particular, is competitive with state-of-the-art AI algorithms and especially stable under the ± 1-class metric (more appropriate for ordinal classifications).

Moreover, in this study, performance is evaluated with respect to the temporal forecasting of an ordinal index, unlike most approaches that focus on fault classification in static scenarios without incorporating the temporal dimension. Therefore, the developed methodology provides a balanced trade-off between accuracy, computational efficiency, and interpretability, directly addressing limitations reported in previous works, and making it suitable for practical deployment in utility maintenance planning.

3.9. Limitations and Future Works

As a limitation of this study, it is noted that the transition and observation models employed represent abstractions of the real behavior of power transformers; however, this does not necessarily constitute a drawback, as it allowed for a more tractable analysis. In addition, the performance of particle filters is strongly influenced by the number of particles N, which creates a balance between accuracy and computational cost. Recursive forecasting, in turn, propagates uncertainties over time. From a computational perspective, runtime grows with N, which reinforces the need to reconcile accuracy with practicality.

As suggestions for future research, it is considered that integrating advanced resampling schemes and adaptive noise strategies could further mitigate particle degeneration in particle filters while preserving computational efficiency.

4. Conclusions

This study presented a hybrid Artificial Intelligence (AI) model incorporating two novel Monte Carlo-based filtering frameworks: AD-Sequential Importance Sampling (AD-SIS) and AD-Bootstrap, which were both developed to enhance probabilistic forecasting and classification in power transformer monitoring systems. The methodology integrated an innovative outlier removal algorithm, based on neighborhood consistency and temporal clustering derived from intervention effectiveness, with probabilistic inference mechanisms tailored to handle noisy and incomplete time-series data.

The experimental results highlighted the superior performance of the AD Bootstrap filter, which achieved 85.45% accuracy across all simulated scenarios. Its effectiveness is attributed to the adaptive resampling mechanism, which mitigates particle degeneracy

and enables dynamic response to abrupt changes in system behavior, such as maintenance interventions.

In contrast, the AD-SIS filter demonstrated reduced generalization capacity under conditions of high variability. This limitation is primarily due to its reliance on fixed importance sampling without resampling, which often results in particle impoverishment and a loss of diversity in the particle set over time. Furthermore, the outlier detection strategy developed in this work outperformed standard approaches such as the Local Outlier Factor (LOF) and Isolation Forest (IF), efficiently filtering inconsistent measurements while preserving critical behavioral patterns and rare anomalies essential for assertive decision making.

The main contributions of this research include the consolidation of heterogeneous diagnostic techniques into a unified and interpretable decision-support framework; the robust identification and treatment of inconsistencies in operational time-series data from the performance index; and the capability to simulate realistic degradation trajectories for preventive maintenance. The developed strategy strengthens both the interpretability and reliability of performance index monitoring, supporting more assertive and individualized maintenance decisions. As a result, the approach offers valuable support to utility companies by enhancing asset management and facilitating intelligent, data-driven decision making with the explicit objective of reducing failure rates and ensuring the continuity of energy supply.

Author Contributions: V.F.C.M., A.P.M., L.S.d.A., J.J.P.d.S., Á.A.C. and C.d.J.R. contributed equally to all aspects of the work, including conceptualization, software, formal analysis, investigation, data curation, writing (original draft preparation and editing), visualization, supervision, project administration, and funding acquisition. All authors have read and agreed to the published version of the manuscript.

Funding: This research was funded by the Research Support Foundation of the State of Goiás (FAPEG).

Institutional Review Board Statement: Not applicable.

Informed Consent Statement: Not applicable.

Data Availability Statement: The dataset used in this study was provided by the High Voltage Engineering Research Laboratory (LAPEAT-UFG). The data are fictitious but technically feasible, having been generated by domain experts to reflect realistic operational conditions of power transformers. This approach ensures technical consistency while safeguarding any sensitive or proprietary information from actual equipment. The dataset is available from the authors upon reasonable request.

Acknowledgments: The authors would like to thank the School of Electrical, Mechanical, and Computer Engineering (EMC) at the Federal University of Goiás (UFG), the High-Voltage Engineering Research Laboratory (LAPEAT-UFG), the Center of Excellence in Wireless Intelligent Networks and Advanced Services (CERISE-UFG), and the Federal Institute of Goiás (IFG) for their support, as well as the Goiás State Research Support Foundation (FAPEG) for funding this work.

Conflicts of Interest: The authors declare no conflicts of interest. The funders had no role in the design of the study; in the collection, analyses, or interpretation of data; in the writing of the manuscript; or in the decision to publish the results.

Abbreviations

The following abbreviations are used in this manuscript:

AI	Artificial Intelligence
AD	Algorithm Designed
AD-Bootstrap	Algorithm Designed Bootstrap Particle Filter
AD-SIS	Algorithm Designed Sequential Importance Sampling filter
AHP	Analytic Hierarchy Process
DBSCAN	Density-Based Spatial Clustering of Applications with Noise
DGA	Dissolved Gas Analysis
DP	Degree of Polymerization
EGML	Expertise-Guided Machine Learning
ESS	Effective Sample Size
ET_CB	Capacitance and Tangent Delta of Condenser Bushings
ET_IR	Insulation Resistance
ET_LVEC	Low-Voltage Excitation Current
ET_PF	Insulation Power Factor
ET_TTR	Turns Transformation Ratio
ET_WR	Winding Resistance
GA	Genetic Algorithms
IF	Isolation Forest
KNN	K-Nearest Neighbors
LOF	Local Outlier Factor
LSTM	Long Short-Term Memory
MEA	Memetic Evolutionary Algorithms
NSE	Not Statistically Effective
PC	Physicochemical Tests
TR1	Power Transformer 1
TR2	Power Transformer 2
TR3	Power Transformer 3
TR4	Power Transformer 4
TR5	Power Transformer 5

References

1. Marques, A.P. Optimized Diagnosis of Power Transformers Through the Integration of Predictive Techniques. Ph.D. Thesis, Federal University of Goiás, Goiânia, Brazil, 2018.
2. Dutta, S.; Dey, J.; Mishra, D.; Baral, A.; Chakravorti, S. Prediction of Insulation Sensitive Parameters of Power Transformer Using Detrended Fluctuation Analysis Based Method. *IEEE Trans. Power Deliv.* **2022**, *37*, 1963–1973. [CrossRef]
3. Nanfak, A.; Eke, S.; Meghnefi, F.; Fofana, I.; Ngaleu, G.M.; Kom, C.H. Hybrid DGA Method for Power Transformer Faults Diagnosis Based on Evolutionary k-Means Clustering and Dissolved Gas Subsets Analysis. *IEEE Trans. Dielectr. Electr. Insul.* **2023**, *30*, 2421–2428. [CrossRef]
4. Liu, H.; Wang, Y.; Chen, W. Anomaly detection for condition monitoring data using auxiliary feature vector and density-based clustering. *IET Gener. Transm. Distrib.* **2020**, *14*, 108–118. [CrossRef]
5. Shen, L.; Du, H.; Liu, S.; Chen, S.; Qiao, L.; Liu, S.; Liu, J.; Li, K.; Li, J. Real time outlier monitoring for power transformer fault diagnosis based on isolated forest. *IOP Conf. Ser. Mater. Sci. Eng.* **2020**, *715*, 12–33. [CrossRef]
6. Zou, D.; Xiang, Y.; Zhou, T.; Peng, Q.; Dai, W.; Hong, Z.; Shi, Y.; Wang, S.; Yin, J.; Quan, H. Outlier detection and data filling based on KNN and LOF for power transformer operation data classification. *Energy Rep.* **2023**, *9*, 698–711. [CrossRef]
7. Feil, D.L.P. Replacement of Power Transformers in Power Substations: A Global Strategy. Ph.D. Thesis, Federal University of Santa Maria, Santa Maria, Brazil, 2019.
8. da Silva, D.G.T. Enhanced Health Index for Power Transformer Diagnosis. Ph.D. Thesis, São Paulo State University, São Paulo, Brazil, 2020.
9. Junior, A.P.P.d.M. Prediction of Power Transformer Failures in Substations Using Finite-State Machines. Master's Thesis, Federal University of Mato Grosso do Sul, Campo Grande, Brazil, 2011.

10. Fehlberg, R.; Carrijo, D.; Gomes, G.; Lopes, S.; Flauzino, R.; Santa Rosa, R.; Patriota, I. Prediction of the Degree of Polymerization Using Machine Learning: A New Methodology for Assessing the Lifespan of Power Transformers. In Proceedings of the XVI Brazilian Symposium on Intelligent Automation and X Brazilian Symposium on Electrical Systems, Manaus, Brazil, October 2023.
11. Zhang, W.; Yang, X.; Deng, Y.; Li, A. An inspired machine-learning algorithm with a hybrid whale optimization for power transformer PHM. *Energies* **2020**, *13*, 31–43. [CrossRef]
12. Kari, T.; Gao, W.; Tuluhong, A.; Yaermaimaiti, Y.; Zhang, Z. Mixed kernel function support vector regression with genetic algorithm for forecasting dissolved gas content in power transformers. *Energies* **2018**, *11*, 24–37. [CrossRef]
13. Wu, Q.; Zhang, H. A novel expertise-guided machine learning model for internal fault state diagnosis of power transformers. *Sustainability* **2019**, *11*, 15–62. [CrossRef]
14. Freeman, C.; Merriman, J.; Beaver, I.; Mueen, A. Experimental comparison and survey of twelve time series anomaly detection algorithms. *J. Artif. Intell. Res.* **2021**, *72*, 849–899. [CrossRef]
15. Assaad, C.K.; Devijver, E.; Gaussier, E. Survey and evaluation of causal discovery methods for time series. *J. Artif. Intell. Res.* **2022**, *73*, 767–819. [CrossRef]
16. Zarezadeh, S.; Asadi, M. Network Reliability Modeling Under Stochastic Process of Component Failures. *IEEE Trans. Reliab.* **2013**, *62*, 917–929. [CrossRef]
17. Cai, Z.; Ma, W.; Wang, X.; Wang, H.; Feng, Z. The Performance Analysis of Time Series Data Augmentation Technology for Small Sample Communication Device Recognition. *IEEE Trans. Reliab.* **2023**, *72*, 574–585. [CrossRef]
18. Abdu, A.; Zhai, Z.; Abdo, H.A.; Algabri, R. Software Defect Prediction Based on Deep Representation Learning of Source Code From Contextual Syntax and Semantic Graph. *IEEE Trans. Reliab.* **2024**, *73*, 820–833. [CrossRef]
19. Dias, Y.A. Method for Predicting the Performance Indices of Power Transformers Immersed in Mineral Insulating Oil and Medium and High-Voltage Circuit Breakers. Ph.D. Thesis, Federal University of Goiás, Goiânia, Brazil, 2023.
20. da Cunha Brito, L.; Marques, A.P.; de Jesus Ribeiro, C.; de Moura, N.K.; Dias, Y.A.; Azevedo, C.H.B.; dos Santos, J.A.L.; da Silva Palhares, P.H. A general methodology for evaluation and classification of oil-immersed power transformers: Application to electrical and physicochemical parameters. *J. Control Autom. Electr. Syst.* **2019**, *30*, 832–839. [CrossRef]
21. Alpaydin, E. *Introduction to Machine Learning*, 3rd ed.; MIT Press: Cambridge, MA, USA, 2014.
22. Alghushairy, O.; Alsini, R.; Soule, T.; Ma, X. A Review of Local Outlier Factor Algorithms for Outlier Detection in Big Data Streams. *Big Data Cogn. Comput.* **2020**, *5*,1.. [CrossRef]
23. Lesouple, J.; Baudoin, C.; Spigai, M.; Tourneret, J.Y. Generalized isolation forest for anomaly detection. *Pattern Recognit. Lett.* **2021**, *149*, 109–119. [CrossRef]
24. Adekunle, A.A.; Oparanti, S.O.; Fofana, I.; Picher, P.; Rodriguez-Celis, E.M.; Arroyo-Fernandez, O.H.; Meghnefi, F. Degradation Mechanisms of Cellulose-Based Transformer Insulation: The Role of Dissolved Gases and Macromolecular Characterisation. *Macromol* **2025**, *5*, 20. [CrossRef]
25. Lundgaard, L.; Hansen, W.; Linhjell, D.; Painter, T. Aging of oil-impregnated paper in power transformers. *IEEE Trans. Power Deliv.* **2004**, *19*, 230–239. [CrossRef]
26. Zhang, E.; Liu, J.; Zhang, C.; Zheng, P.; Nakanishi, Y.; Wu, T. State-of-Art Review on Chemical Indicators for Monitoring the Aging Status of Oil-Immersed Transformer Paper Insulation. *Energies* **2023**, *16*, 1396. [CrossRef]
27. Montero, A.; García, B.; López, C. Life Expectancy of Transformer Paper Insulation Retrofilled with Natural Ester in the Laboratory. *Polymers* **2023**, *15*, 4345. [CrossRef]
28. Feng, D.; Wang, Z.; Jarman, P. Modeling thermal life expectancy of the UK transmission power transformers. In Proceedings of the 2012 International Conference on High Voltage Engineering and Application, Shanghai, China, 17–20 September 2012; pp. 540–543. [CrossRef]
29. Feng, D.; Hao, J.; Liao, R.; Chen, X.; Cheng, L.; Liu, M. Comparative Study on the Thermal-Aging Characteristics of Cellulose Insulation Polymer Immersed in New Three-Element Mixed Oil and Mineral Oil. *Polymers* **2019**, *11*, 1292. [CrossRef]
30. Seifaddini, N.; Fofana, I.; Rajesh Kandala, N.; Lim, K.S.; Ooi, C.W.; Udos, W.; Sekongo, B.; Chehri, A.; Ouhrouche, M.; Leena, G. Aging characterization of thermally aged transformer paper based on its reflectance. *Results Opt.* **2024**, *16*, 100716. [CrossRef]
31. Silva, F.C.d. Bayesian Sequential Monte Carlo Methods: Computational, Inferential, and Applied Aspects. Ph.D. Thesis, Federal University of Minas Gerais, Belo Horizonte, Brazil, 2016.
32. Doucet, A.; de Freitas, N.; Gordon, N. (Eds.) *Sequential Monte Carlo Methods in Practice*; Springer: New York, NY, USA, 2001.
33. Elvira, V.; Miguez, J.; Djurić, P.M. On the performance of particle filters with adaptive number of particles. *Stat. Comput.* **2021**, *31*, 81. [CrossRef]
34. Akyildiz, Ö.D.; Míguez, J. Nudging the particle filter. *Stat. Comput.* **2020**, *30*, 305–330. [CrossRef]
35. Chen, X.; Li, Y. An overview of differentiable particle filters for data-adaptive sequential Bayesian inference. *Foundations of Data Science*, early access, December 2023. [CrossRef]
36. Zhao, F.; Cai, R. Adaptive particle filter for state estimation with application to non-linear system. *IET Signal Process.* **2022**, *16*, 1023–1033. [CrossRef]

37. Aspeel, A.; Gouverneur, A.; Jungers, R.M.; Macq, B. Optimal Intermittent Particle Filter. *IEEE Trans. Signal Process.* **2022**, *70*, 2814–2825. [CrossRef]
38. Elfring, J.; Torta, E.; van de Molengraft, R. Particle Filters: A Hands-On Tutorial. *Sensors* **2021**, *21*, 438. [CrossRef]
39. Shahapure, K.R.; Nicholas, C. Cluster Quality Analysis Using Silhouette Score. In Proceedings of the 2020 IEEE 7th International Conference on Data Science and Advanced Analytics (DSAA), Sydney, Australia, 6–9 October 2020; pp. 747–748. [CrossRef]
40. Mulyani, H.; Setiawan, R.A.; Fathi, H. Optimization of K Value in Clustering Using Silhouette Score (Case Study: Mall Customers Data). *J. Inf. Technol. Its Util.* **2023**, *6*, 45–50. [CrossRef]
41. Pedregosa, F.; Varoquaux, G.; Gramfort, A.; Michel, V.; Thirion, B.; Grisel, O.; Blondel, M.; Prettenhofer, P.; Weiss, R.; Dubourg, V.; et al. Scikit-learn: Machine Learning in Python. *J. Mach. Learn. Res.* **2011**, *12*, 2825–2830.
42. Buitinck, L.; Louppe, G.; Blondel, M.; Pedregosa, F.; Mueller, A.C.; Grisel, O.; Niculae, V.; Prettenhofer, P.; Gramfort, A.; Grobler, J.; et al. API design for machine learning software: Experiences from the scikit-learn project. In Proceedings of the ECML PKDD Workshop: Languages for Data Mining and Machine Learning, Prague, Czech Republic, 23–27 September 2013; pp. 108–122.
43. Varoquaux, G.; Buitinck, L.; Louppe, G.; Grisel, O.; Pedregosa, F.; Mueller, A. Scikit-learn. *GetMobile Mob. Comput. Commun.* **2015**, *19*, 29–33. [CrossRef]
44. Barbosa, F.R.; Almeida, O.M.; Braga, A.P.S.; Amora, M.A.B.; Cartaxo, S.J.M. Application of an artificial neural network in the use of physicochemical properties as a low cost proxy of power transformers DGA data. *IEEE Trans. Dielectr. Electr. Insul.* **2012**, *19*, 239–246. [CrossRef]
45. Miranda, V.; Castro, A.R.G.; Lima, S. Diagnosing faults in power transformers with autoassociative neural networks and mean shift. *IEEE Trans. Power Deliv.* **2012**, *27*, 1350–1357. [CrossRef]
46. Ghoneim, S.S.M.; Taha, I.B.M.; Elkalashy, N.I. Integrated ANN-based proactive fault diagnostic scheme for power transformers using dissolved gas analysis. *IEEE Trans. Dielectr. Electr. Insul.* **2016**, *23*, 1838–1845. [CrossRef]
47. Yang, D.; Qin, J.; Pang, Y.; Huang, T. A Novel Double-Stacked Autoencoder for Power Transformers DGA Signals With an Imbalanced Data Structure. *IEEE Trans. Ind. Electron.* **2022**, *69*, 1977–1987. [CrossRef]
48. Baker, E.; Nese, S.V.; Dursun, E. Hybrid Condition Monitoring System for Power Transformer Fault Diagnosis. *Energies* **2023**, *16*, 1151. [CrossRef]
49. Gorginpour, H.; Ghimatgar, H.; Toulabi, M.S. Lifetime Estimation and Optimal Maintenance Scheduling of Urban Oil-Immersed Distribution-Transformers Considering Weather-Dependent Intelligent Load Model and Unbalanced Loading. *IEEE Trans. Power Deliv.* **2022**, *37*, 4154–4165. [CrossRef]
50. Senoussaoui, M.E.A.; Brahami, M.; Fofana, I. Transformer Oil Quality Assessment Using Random Forest with Feature Engineering. *Energies* **2021**, *14*, 1809. [CrossRef]
51. Harbaji, M.; Shaban, K.; El-Hag, A. Classification of common partial discharge types in oil-paper insulation system using acoustic signals. *IEEE Trans. Dielectr. Electr. Insul.* **2015**, *22*, 1674–1683. [CrossRef]
52. Kunicki, M.; Wotzka, D. A Classification Method for Select Defects in Power Transformers Based on the Acoustic Signals. *Sensors* **2019**, *19*, 5212. [CrossRef]
53. Ilyushin, Y.; Nosova, V.; Krauze, A. Application of Systems Analysis Methods to Construct a Virtual Model of the Field. *Energies* **2025**, *18*, 1012. [CrossRef]